Tunable transport properties of *n*-type ZnO nanowires by Ti plasma immersion ion implantation

L. Liao,[1] Z. Zhang,[1] Y. Yang,[2] B. Yan,[1] H. T. Cao,[2] L. L. Chen,[2] G. P. Li,[1] T. Wu,[1] Z. X. Shen,[1] B. K. Tay,[2] T. Yu,[1,a)] and X. W. Sun[2,b)]
[1]*Division of Physics and Applied Physics, School of Physical and Mathematical Sciences, Nanyang Technological University, Singapore 637371, Singapore*
[2]*School of Electrical and Electronic Engineering, Nanyang Technological University, Singapore 639798, Singapore*

(Received 9 July 2008; accepted 26 July 2008; published online 7 October 2008)

Single-crystalline, transparent conducting ZnO nanowires were obtained simply by Ti plasma immersion ion implantation (PIII). Electrical transport characterizations demonstrate that the *n*-type conduction of ZnO nanowire could be tuned by appropriate Ti-PIII. When the energy of PIII is increased, the resistivity of ZnO decreases from 4×10^{2} to 3.3×10^{-3} Ω cm, indicating a semiconductor-metal transition. The failure-current densities of the metallic ZnO could be up to 2.75×10^{7} A/cm^2. Therefore, this facile method may provide an inexpensive alternative to tin doped indium oxide as transparent conducting oxide materials. © *2008 American Institute of Physics*. [DOI: 10.1063/1.2981189]

Transparent conducting oxides (TCOs) are a unique group of materials that offer both high optical transmissivity in the visible range and low electrical resistivity. Common TCO materials include donor-doped oxides such as SnO_2,[1] In_2O_3,[2] ZnO,[3] and their ternary alloys, with tin doped indium oxide (ITO) being the most widely used TCO material. The uncertain supply of indium, however, has led to urgent needs for low-cost alternatives such as ZnO-based TCO materials in large-scale applications including flat panel displays, solar cells, and light-emitting diodes.[4–6]

Recently, ZnO, a multifunctional semiconducting material with a wide-direct bandgap (3.37 eV at room temperature) and large exciton binding energy (60 meV), has stirred new interest as a promising nanoelectronic material in UV lasers,[7] light-emitting diodes,[6] and gas sensor.[8] For ZnO nanostructures, group III elements (Al, Ga, or In) are commonly used to substitute Zn in order to enhance *n*-type conductivity. The success of doping is often accompanied and characterized by changes in optical and electrical properties of ZnO nanostructures.[3] Therefore, it is important to develope fascile methods for doping ZnO.

In this letter, the electrical properties of ZnO nanowires (NWs) post-treated by Ti plasma immersion ion implantation (PIII) were characterized using single NW field-effect transistors (FETs). The variation in electron concentration in Ti-doped ZnO NWs was dictated by the implantation conditions. Importantly, metallic ZnO NWs could be obtained by using this facile method.

The ZnO NWs were grown by a vapor phase transport method in a horizontal tube furnace. ZnO (99.99%, Alfa Aesar) and graphite powders (99.99%, Aldrich) (1:1 wt %) on the Si (111) substrate precoated with a 20 nm Au film. The source was maintained at 950 °C for 10 min for the NW growth.

As-grown ZnO NWs were removed by sonication from the substrates, and subsequently dispersed into ethanol. The solution was dripped on SiO_2/Si (i.e., a 200 nm thick insulating SiO_2 film on Si), and then Au contact pads of 100 nm thick were fabricated by photolithography and rf sputtering. The nanodevices were then directly treated with Ti-PIII. Negative pulse voltage of 5 and 10 kV were applied on the substrate holder for 2 min. The ion dose was estimated to be about 5×10^{14} ions/cm^2. In order to get good Ohmic contacts, the devices were annealed at 350 °C for 1 h.

The morphologies and microstructures of ZnO NWs were characterized by scanning electron microscopy (SEM) (JEOL JSM-6700F) and transmission electron microscopy (TEM) (200 kV JEOL 2010F). The chemical composition analysis was carried out using energy dispersive x-ray spectroscopy (EDX). The photoluminescence spectra were measured using a He–Cd laser (325 nm) and a confocal Renishaw Raman microscope (40× lens) at room temperature. The spot size is 1.0 μm. The excitation power density is 1.27×10^{3} W/cm^2. The electrical transport properties were measured by using a Suss probe station with Keithley 4200 SCS.

Figures 1(a) and 1(c) show the typical TEM images of ZnO NW before and after 10 kV Ti-PIII, respectively. The insets are the corresponding selected area electron diffraction (SAED) patterns. Figures 1(b) and 1(d) are the high-resolution TEM (HRTEM) images corresponding to the NWs in Figs. 1(a) and 1(c), respectively. No visible linear or planer defects were observed from the HRTEM image of the as-grown ZnO NW. The *d*-spacing of 0.26 nm corresponds to lattice spacing of (0001) planes of wurtzite ZnO. Figure 1(d) shows the HRTEM of the ZnO surface after the 10 kV ion treatment. The clear extension and continuity of the lattice planes from the body to the surface proves that no Ti-related coating layer or new crystalline phases such as TiO_2 were introduced by PIII. Moreover, ZnO NWs treated under 5 kV bias exhibit the similar structural characteristics, implying that the Ti ion could be readily implanted into ZnO NWs

a)Author to whom correspondence should be addressed. Electronic mail: yuting@ntu.edu.sg. URL: www.ntu.edu.sg/home/yuting.
b)Electronic mail: xwsun@ntu.edu.sg.

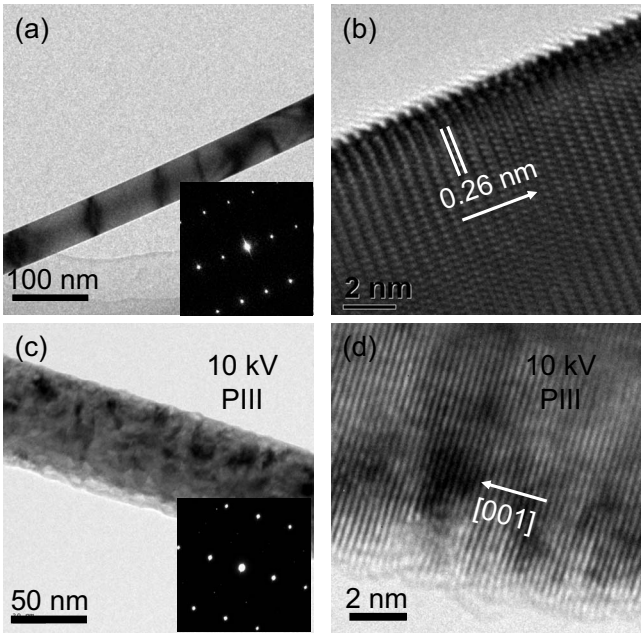

FIG. 1. [(a) and (c)] Typical low-magnification TEM images of ZnO NWs before and after 10 kV Ti-PIII, respectively. Insets are the corresponding SAED patterns. [(b) and (d)] HRTEM images of the corresponding ZnO NWs.

under a relatively low energy plasma immersion process. To confirm that Ti was indeed present in ZnO NWs, EDX was carried out to investigate the elemental composition of ZnO NWs. The Ti concentration is less than 1% in ZnO NWs.[9]

The SEM image and the schematic device diagram of a single ZnO NW FET are shown in Fig. 2(a) and the inset, respectively. The optical properties of the Ti-PIII modified ZnO nanostructures have been reported in *our* pervious studies.[9,10] The corresponding PL spectra of a single ZnO NW after Ti-PIII surface modification are shown in Fig. 2(b). For the as-grown ZnO NW, relatively weak near-bandgap emission can be seen at 3.3 eV accompanied by a broad and strong green band (GB) emissions peaking around 2.2 eV. The GB emission is significant in all the nanodevices after the microfabrication. However, the single ZnO NW showed quenching of the GB emission after the PIII treatments. The origin of GB has been studied extensively, and is generally attributed to the radiative transition involving native surface defects such as singly ionized oxygen vacancies (V_O).[11] It is

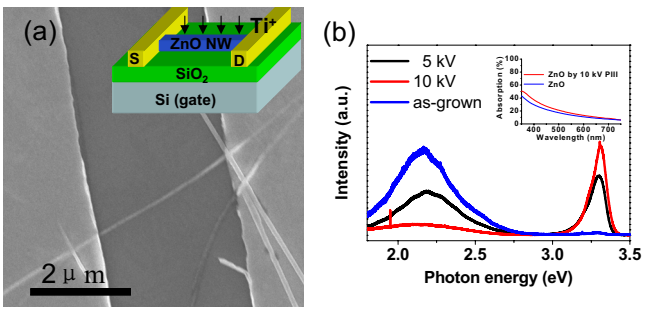

FIG. 2. (Color online) (a) S chematic diagram and SEM image of a single ZnO NW FET. (b) PL spectra of the as-grown ZnO NW and the ZnO NWs after different Ti-PIII treatments. The insets show the absorption of ZnO NWs before and after 10 kV Ti-PIII.

worth noting that the ZnO NWs on quartz substrate after Ti-PIII are still highly transparent in the visible range, almost the same as the as-grown ZnO NWs, as shown in the inset of Fig. 2(b). The absorption is below 40% between 400 and 750 nm.

Figure 3(a) shows I_{ds} versus V_{ds} curves obtained from the devices made of the as-grown ZnO NWs under various V_g varying from −10 to 10 V. The linear I_{ds}-V_{ds} curves indicate that the Au electrodes form good Ohmic contacts with the as-grown ZnO NWs. The I_{ds} versus V_g curves for the as-grown ZnO NW recorded at different V_{ds} are shown in Fig. 3(d), which shows clearly a threshold voltage about −20 V and an on/off ratio as large as 10^5. The resistivity measured at $V_g=0$ is about 4×10^2 Ω cm. The typical characteristics of a *n*-channel semiconductor FET can also be observed. According to previous studies on ZnO thin films,[12] the *n*-type behavior usually observed in the as-grown ZnO NWs is due to intrinsic donor defects, such as V_O. Following the standard procedure,[13] the electron concentration of the as-grown NWs is estimated to be $n=2.5\times10^8$ cm^{-1}, corresponding to a 4.8×10^{18} cm^{-3}. The mobility is $\mu_e=\sim15$ cm^2/V s, which is comparable to the value ($\sim10^{17}$–10^{18} cm^{-3}).[14]

Similar FETs were also measured after Ti-PIII modifications. For ZnO NW modified by 5 kV PIII, the I_{ds}-V_{ds} curves for different V_g also confirm the *n*-type behavior, as depicted in Fig. 3(b). Significantly, the resistivity measured at $V_g=0$ decreases from 4×10^2 to 1×10^{-2} Ω cm after doping Ti ion into ZnO NWs, which demonstrates that the resistance of ZnO NWs can be effectively tuned by Ti-PIII. Furthermore, the NW device cannot be turned off at $V_g=-30$ V [Fig. 3(e)]. The mobility of these Ti-doped ZnO NWs was calculated to be about 25 cm^2/V s, and the electron concentration about 5.8×10^{19} cm^{-3}, one order of magnitude higher than that of the as-grown ZnO NW. The observation of this higher mobility in doped ZnO NWs is contrary to what is usually observed in semiconductor materials, for example, mobility usually decreases with increasing dopant concentration.[15] In the present case, the increased mobility is possibly due to the compensation of intrinsic defects by Ti ions,[10] which may reduce the trapping and scattering of carriers.

With further increasing Ti-PIII energy to 10 keV, it is clear that under the same V_{ds}, I_{ds} increases by two orders of magnitude relative to that of the as-grown ZnO NWs, as shown in Fig. 3(c). This NW has a low resistivity of 3.3×10^{-3} Ω cm, and the I_{ds}-V_{ds} curves show no dependence on V_g, and the *I*-*V* curves recorded at V_g of −10, −5, 0, 5, and 10 V are almost overlapping. Because of the lack in information on electron mobility, it is impossible to accurately calculate the electron concentration in the 10 kV PIII treated ZnO NWs by using the above method. However, an electron concentration in the order of 10^{20} cm^{-3} can be roughly estimated from the resistivity values. Moreover, the I_{ds}-V_g curve indicates that the Ti-doped ZnO NW behaves metallic, as shown in Fig. 3(f).

Due to the single-crystalline nature, these "metallic" Ti-doped ZnO NWs can also carry a very high current density. As shown in Fig. 4, the NW can endure a current up to 0.55 mA, corresponding to a failure-current density J_c of 2.75

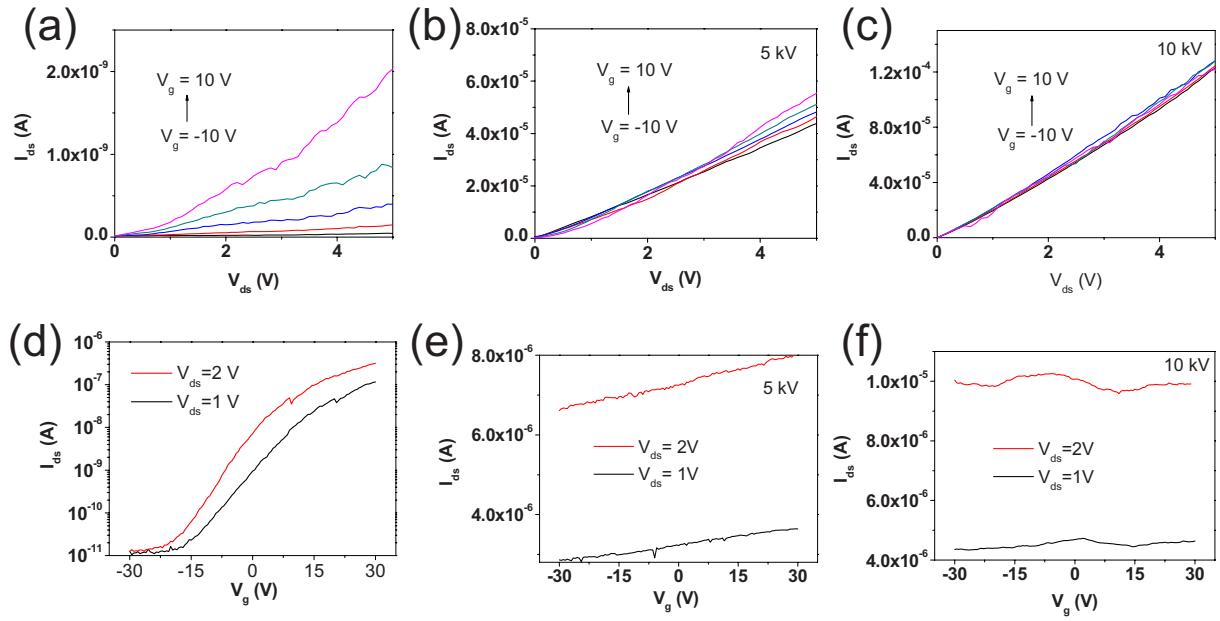

FIG. 3. (Color online) [(a)–(c)] I_{ds}-V_{ds} curves of single as-grown ZnO NW and ZnO NW at different Ti-PIII treatments. [(d)–(f)] I_{ds}-V_g curves of single as-grown ZnO NW and ZnO NW at different Ti-PIII statuses.

$\times 10^7$ A/cm^2, which is an order of magnitude higher than observed in lithographically defined noble metal lines.[16] The inspection of the failed Ti-doped ZnO NW device (inset) revealed that the failure was likely caused by melting due to resistive self-heating.

According to our results, the conductivity of Ti-PIII treated ZnO NW increases with the increase in implantation energy. However, the dose of the Ti-PIII did not change, so activated dopants spread out in a wider area resulting in higher conductivity. For thin films, doping of cations of higher valence state than Zn (Zn^{2+}) into ZnO, such as Al, Ga, and Ni, leads to an increase in the electrical conductivity.[3,17] Compared to the as-grown ZnO NW, the doped Ti enhances the conductivity probably due to the presence of Ti^{3+} or Ti^{4+} cations, which would contribute free electrons, and act as shallow donors

In conclusion, we developed a facile method to obtain single-crystalline, metallic, and transparent ZnO NW. By introducing an energy controllable Ti-PIII, electrical transport properties of *n*-type ZnO NW could be readily tuned from semiconducting to metallic, associating with the resistivity decreasing from 4×10^2 to 3.3×10^{-3} Ω cm. The failure-current density of the metallic ZnO NWs is as high as 2.75 $\times 10^7$ A/cm^2. This work may help facilitate the development of ZnO as TCO materials in advanced applications.

Liao Lei acknowledges the support by the Singapore Millennium Foundation 2008 scholarship.

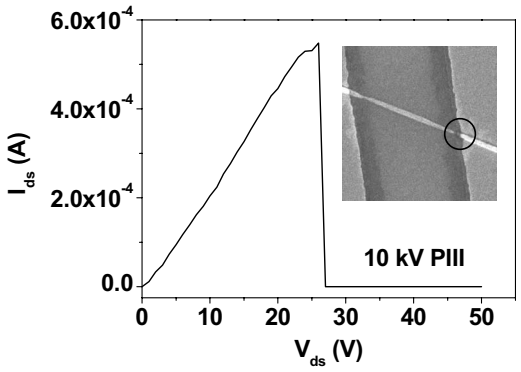

FIG. 4. I_{ds}-V_{ds} curve for the same nanowire at large biases. Inset: SEM image of the failed ZnO NW, showing the failure site.

[1] Q. Wan, E. N. Dattoli, and W. Lu, Appl. Phys. Lett. **90**, 222107 (2007).
[2] Q. Wan, E. N. Dattoli, W. Y. Fung, W. Guo, Y. B. Chen, X. Q. Pan, and W. Lu, Nano Lett. **6**, 2909 (2006).
[3] G. D. Yuan, W. J. Zhang, J. S. Jie, X. Fan, J. X. Tang, I. Shafiq, Z. Z. Ye, C. S. Lee, and S. T. Lee, Adv. Mater. (Weinheim, Ger.) **20**, 168 (2008).
[4] L. Liao, J. C. Li, D. H. Liu, C. Liu, D. F. Wang, W. Z. Song, and Q. Fu, Appl. Phys. Lett. **86**, 083106 (2005).
[5] M. Law, L. E. Greene, J. C. Johnson, R. Saykally, and P. D. Yang, Nat. Mater. **4**, 455 (2005).
[6] X. W. Sun, J. Z. Huang, J. X. Wang, and Z. Xu, Nano Lett. **8**, 1219 (2008).
[7] M. H. Huang, S. Mao, H. Feick, H. Q. Yan, Y. Y. Wu, H. Kind, E. Weber, R. Russo, and P. D. Yang, Science **292**, 1897 (2001).
[8] L. Liao, H. B. Lu, J. C. Li, C. Liu, D. J. Fu, and Y. L. Liu, Appl. Phys. Lett. **91**, 173110 (2007).
[9] Y. Yang, B. K. Tay, X. W. Sun, J. Y. Sze, Z. J. Han, J. X. Wang, X. H. Zhang, Y. B. Li, and S. Zhang, Appl. Phys. Lett. **91**, 071921 (2007).
[10] Y. Yang, X. W. Sun, B. K. Tay, P. H. T. Cao, J. X. Wang, and X. H. Zhang, J. Appl. Phys. **103**, 064307 (2008).
[11] N. E. Hsu, W. K. Hung, and Y. F. Chen, J. Appl. Phys. **96**, 4671 (2004).
[12] P. F. Carcia, R. S. McLean, M. H. Reilly, M. K. Crawford, E. N. Blanchard, A. Z. Kattamis, and S. Wagner, J. Appl. Phys. **102**, 074512 (2007).
[13] P. C. Chang, Z. Y. Fan, C. J. Chien, D. Stichtenoth, C. Ronning, and J. G. Lu, Appl. Phys. Lett. **89**, 133113 (2006).
[14] B. Xiang, P. Wang, X. Zhang, S. Dayeh, D. Aplin, C. Soci, D. P. Yu, and D. L. Wang, Nano Lett. **7**, 323 (2007).
[15] S. M. Sze, *Physics of Semiconductor Devices* (Wiley, New York, 1981).
[16] Y. Wu, J. Xiang, C. Yang, W. Lu, and C. M. Lieber, Nature (London) **430**, 61 (2004).
[17] J. H. He, C. S. Lao, L. J. Chen, D. Davidovic, and Z. L. Wang, J. Am. Chem. Soc. **127**, 16376 (2005).